Neuron, Vol. 43, 563–574, August 19, 2004, Copyright ©2004 by Cell Press

SynGAP-MUPP1-CaMKII Synaptic Complexes Regulate p38 MAP Kinase Activity and NMDA Receptor-Dependent Synaptic AMPA Receptor Potentiation

Grigory Krapivinsky,[1] Igor Medina,[2] Luba Krapivinsky,[1] Svetlana Gapon,[1] and David E. Clapham[1,*]

[1]Howard Hughes Medical Institute
Children's Hospital
1309 Enders Building
320 Longwood Avenue
Boston, Massachusetts 02115

[2]INMED/INSERM Unite 29
163 Route de Luminy
13009 Marseille
France

Summary

The synapse contains densely localized and interacting proteins that enable it to adapt to changing inputs. We describe a Ca^{2+}-sensitive protein complex involved in the regulation of AMPA receptor synaptic plasticity. The complex is comprised of MUPPI, a multi-PDZ domain-containing protein; SynGAP, a synaptic GTPase-activating protein; and the Ca^{2+}/calmodulin-dependent kinase CaMKII. In synapses of hippocampal neurons, SynGAP and CaMKII are brought together by direct physical interaction with the PDZ domains of MUPP1, and in this complex, SynGAP is phosphorylated. Ca^{2+}/CaM binding to CaMKII dissociates it from the MUPP1 complex, and Ca^{2+} entering via the NMDAR drives the dephosphorylation of SynGAP. Specific peptide-induced SynGAP dissociation from the MUPP1-CaMKII complex results in SynGAP dephosphorylation accompanied by P38 MAPK inactivation, potentiation of synaptic AMPA responses, and an increase in the number of AMPAR-containing clusters in hippocampal neuron synapses. siRNA-mediated SynGAP knockdown confirmed these results. These data implicate SynGAP in NMDAR- and CaMKII-dependent regulation of AMPAR trafficking.

Introduction

Hippocampal learning and memory rely on activity-dependent synaptic plasticity. In the long-term potentiation (LTP) and depression (LTD) models of synaptic plasticity, brief periods of repetitive synaptic activity lead to sustained changes in synaptic transmission. The critical events in plasticity are NMDA receptor activation and the elevation of postsynaptic [Ca^{2+}] during repetitive synaptic activity. Recent studies argue that the NMDAR-dependent trafficking of postsynaptic AMPA-sensitive glutamate receptors (AMPAR) is a key element in plasticity (Luscher et al., 1999; Shi et al., 1999; Hayashi et al., 2000; Lu et al., 2001; Zhu et al., 2002; see Malinow, 2003, for a recent review). Ca^{2+}/calmodulin-dependent kinase II (CaMKII), the small Ras family GTPases Ras and Rap, ERK and p38 MAP kinases, PI3 kinase, and other molecules participate in the regulation of NMDAR-dependent AMPA receptor trafficking to synapses (Zhu et al., 2002; Man et al., 2003). Overexpression of dominant-negative and constitutively active forms of small GTPases supports the notion that a Ras-dependent pathway increases, while a Rap-dependent pathway decreases, the number of active AMPARs in postsynaptic membranes (Zhu et al., 2002). However, the molecular mechanisms linking NMDA receptor activation with Ras and Rap GTPases are poorly understood.

Two Ca^{2+}-dependent signaling Ras effector molecules, RasGRF1 and SynGAP, are candidates for linking NMDA receptor activation and Ca^{2+} influx with Ras GTPases (Platenik et al., 2000). Recently, we showed that the Ca^{2+}/CaM-dependent GTP/GDP exchanger RasGRF1 was responsible for NMDAR (NR2B)-dependent activation of ERK kinases (Krapivinsky et al., 2003), but what is the Ca^{2+}-dependent role of SynGAP? SynGAP is localized to postsynaptic densities (Chen et al., 1998; Kim et al., 1998) and phosphorylated in vitro by Ca^{2+}-dependent CaMKII. Controversial in vitro data suggested that direct SynGAP phosphorylation by CaMKII regulated its activity (Chen et al., 1998; Oh et al., 2002; Oh et al., 2004). Multiple SynGAP splice variants have been found (Kim et al., 1998; Li et al., 2001). SynGAP-α has a PDZ binding motif on its C terminus and does not directly bind CaMKII; SynGAP-β lacks a C-terminal PDZ binding consensus and directly binds CaMKII (Li et al., 2001). Disruption of the SynGAP gene results in postnatal lethality, while heterozygous mice display defects in LTP (Komiyama et al., 2002; Kim et al., 2003). Clearly, SynGAP plays an important role in the synapse.

The tethering of signaling molecules within the NMDAR complex localizes them to the high [Ca^{2+}] domain near the channel pore and organizes Ca^{2+}-activated downstream responses. Scaffolding molecules such as PSD-95 structurally organize macromolecular complexes in the postsynaptic density (Sheng and Sala, 2001). MUPP1, a large, ubiquitously expressed scaffolding protein, contains 13 homologous protein binding PDZ domains (Ullmer et al., 1998). Not surprisingly, MUPP1 interacts with many proteins, including the tight junction claudins (Poliak et al., 2002), tyrosine kinase receptors (Mancini et al., 2000), PIP_2 binding proteins (Kimber et al., 2002), serotonin receptors (Parker et al., 2003), and neuronal Rho-GEF (Penzes et al., 2001).

Here we show that MUPP1 is a component of the NMDAR signaling complex in excitatory synapses of hippocampal neurons. Within this complex, MUPP1 directly binds SynGAP-α and CaMKII. Calmodulin binding dissociates CaMKII from the complex. In dormant neurons, SynGAP is phosphorylated in a CaMKII-dependent fashion. Upon NMDAR stimulation, Ca^{2+} entering the synapse dissociates CaMKII, and SynGAP is dephosphorylated. Disruption of the MUPP1-SynGAP complex with competitive peptides also results in SynGAP dephosphorylation, attenuates p38 MAP kinase activity, and increases the number of synapses containing func-

*Correspondence: dclapham@enders.tch.harvard.edu

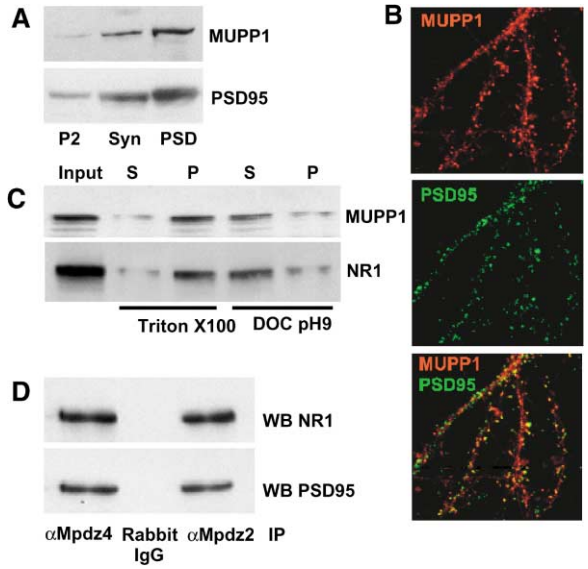

Figure 1. MUPP1 Is a Component of the NMDAR Synaptic Complex

(A) MUPP1 is enriched in postsynaptic densities (PSDs). Protein (10 μg) from rat brain P2 membrane, purified synaptosomes (Syn), and PSDs were probed by Western blot with Mpdz4 and PSD-95 antibodies. The amount of MUPP1 in PSDs increased in parallel with the PSD protein marker PSD-95.

(B) MUPP1 colocalized with PSD-95 in synapses of rat hippocampal neurons (18 d.i.v.). Neurons were labeled with αMpdz4 (red) and αPSD-95 (green).

(C) Both MUPP1 and NR1 were predominantly in the pellet (P) of synaptosomal membranes extracted with Triton X-100 and almost completely solubilized (S) with alkaline sodium deoxycholate (DOC).

(D) Two different MUPP1 antibodies coimmunoprecipitated the NMDAR subunit, NR1, and PSD-95 from solubilized synaptosomes. After probing with NR1 antibody, the blot was stripped and reprobed with PSD-95 antibody.

tional AMPA receptors. SynGAP is thus a crucial link in NMDAR-dependent control of AMPAR trafficking.

Results

MUPP1 Directly Interacts with SynGAP-α

MUPP1 is highly expressed in brain and displays distinct expression patterns, including hippocampal localization (Sitek et al., 2003). Whole rat brain fractionation revealed that MUPP1 is highly enriched in the synaptosomes, specifically in postsynaptic densities (PSD) (Figure 1A). MUPP1 was localized to punctae on dendrites of cultured rat hippocampal neurons and colocalized with the synaptic marker PSD-95 (Figure 1B). Synaptosomal MUPP1 was not extractable with 2% Triton X-100 but was significantly solubilized with alkaline (pH 9.0) 1% sodium cholate (Figure 1C). Since MUPP1 solubility was similar to the solubility of the NMDAR complex (Lau et al., 1996), we reasoned that it might be a component of this complex. In fact, the NR1 subunit of NMDA receptor and PSD-95, a component of the NMDAR complex (Kornau et al., 1995), specifically coimmunoprecipitated with MUPP1 (Figure 1D). This coimmunoprecipitation was blocked when MUPP1 antibodies were preabsorbed with specific antigens (data not shown).

The NMDAR complex contains numerous structural and signaling molecules (Husi et al., 2000). To determine which molecules might interact with MUPP1, a yeast two-hybrid screen of a human brain library was completed using multiple separate PDZ domains of MUPP1 as baits. A bait containing PDZ13 recovered five independent cDNA clones encoding the C-terminal portion of the synaptic RasGAP SynGAP-α. The shortest clone encoded a protein sequence that was identical to the last 111 amino acids of rat SynGAP-α (called SynGAP hereafter, accession number AF058790).

The interaction of MUPP1 and SynGAP was probed in vitro. The GST-tagged PDZ13 domain of MUPP1 and the His-tagged C-terminal 111 amino acids of SynGAP, expressed in bacteria and affinity purified, directly and specifically bound each other (Figure 2A). A GST fusion protein of the MUPP1 ninth PDZ domain did not bind SynGAP and served as the control. Full-length HA-tagged SynGAP and FLAG-tagged MUPP1 coexpressed in HEK293T cells formed a complex that coimmunoprecipitated SynGAP with MUPP1 (Figure 2B). Finally, MUPP1 and SynGAP were coimmunoprecipitated from solubilized rat brain microsomes (Figure 2C) and from 14-day-old primary cultures of dissociated rat neonatal hippocampal neurons (data not shown). These data suggest that PDZ13 of MUPP1 and SynGAP directly associate to form a molecular complex in native neurons.

MUPP1 and SynGAP Binding Domains

To determine functions that depend on the MUPP1-SynGAP interaction in live neurons, we developed tools to specifically disrupt this interaction. The advantage of this approach, as compared to disrupting the gene or overexpressing the protein, is that the interaction can be specifically targeted in vivo, without disturbing other components of the system or resulting in longer-term compensatory changes. Interacting fragments on both MUPP1 and SynGAP molecules were identified, and the peptides encoding these interacting fragments were tested for their ability to interfere with the MUPP1-SynGAP interaction. We employed the TAT peptide delivery system to incorporate TAT fusion proteins into entire populations of living neurons within minutes (for review, see Wadia and Dowdy, 2003).

The SynGAP C terminus contains the PDZ recognition motif QTXV (Hung and Sheng, 2002). To determine if this motif was essential for the interaction with MUPP1, we performed a pull-down assay of in vitro-translated SynGAP fragments with GST-PDZ13. Truncation of the last three amino acids of SynGAP significantly reduced but did not completely abolish the interaction of GST-PDZ13 with SynGAP (Supplemental Figure S1A [http://www.neuron.org/cgi/content/full/43/4/563/DC1]). This suggested that the region upstream of the canonical QTXV sequence may be important for stronger binding and specificity, allowing SynGAP to preferentially bind one PDZ domain among the many that are present. We tested this possibility in competition experiments. Fragments of the SynGAP C terminus were translated in vitro and tested for their potency in inhibiting the interaction of in vitro-translated full-length MUPP1 and SynGAP. Fusion proteins containing SynGAP (C terminal 33, 49, and 75 amino acids) did not inhibit the MUPP1-SynGAP interaction in vitro, and only the fragment con-

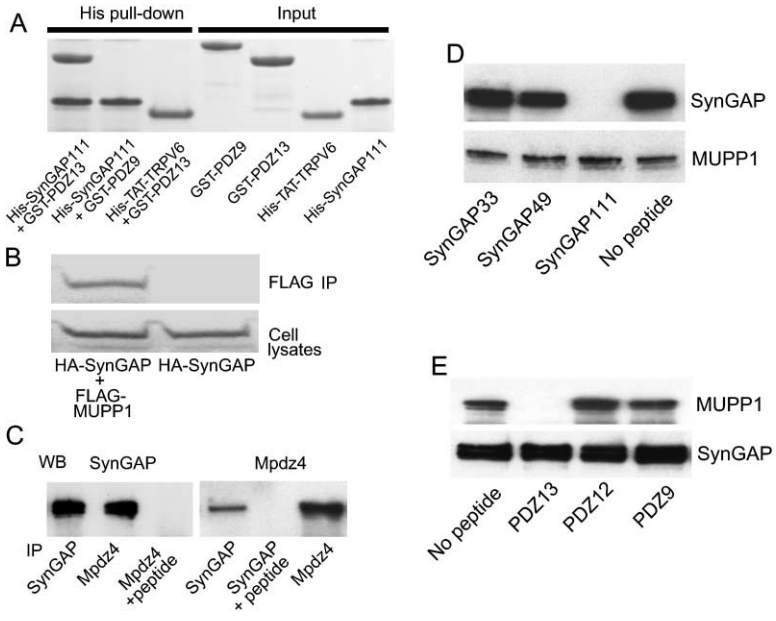

Figure 2. MUPP1 and SynGAP Interact In Vitro and In Vivo

(A) Purified His-tagged SynGAP fragment containing 111 C-terminal amino acids (His-SynGAP111) specifically binds the MUPP1 thirteenth PDZ domain (fused with GST, GST-PDZ13) in pull-down assays. The ninth PDZ domain (GST-PDZ9) of MUPP1 and a His-TAT-tagged fragment of TRPV6 served as negative controls (Coomassie-stained gel).

(B) Interaction of full-length FLAG-MUPP1 and HA-SynGAP coexpressed in HEK293T cells. The cell lysate was immunoprecipitated with FLAG antibody and probed with αHA.

(C) MUPP1 and SynGAP coimmunoprecipitated from solubilized rat brain synaptosomes. This coimmunoprecipitation was blocked when the immunoprecipitating antibody was preabsorbed with the appropriate antigenic peptide.

(D) TAT-SynGAP111 disrupted the MUPP1-SynGAP interaction in the native complex. MUPP1 was immunoprecipitated from rat brain synaptosomes with αMpdz4 in the presence of 5 μM TAT-SynGAP C-terminal fusion peptides. Coimmunoprecipitated SynGAP was detected by Western blot (TAT-SynGAP75 failed to express in bacteria and was not tested).

(E) TAT-PDZ13 disrupted the MUPP1-SynGAP interaction in the native complex. SynGAP was immunoprecipitated from rat brain synaptosomes with SynGAP antibody in the presence of 5 μM TAT-PDZ fusion peptides.

taining the 111 C-terminal amino acids (SynGAP111) completely disrupted it (Supplemental Figure S1B). The same pattern of peptide potency was observed in the disruption of native molecule interactions. TAT-SynGAP111 specifically disrupted coimmunoprecipitation of the MUPP1-SynGAP from the native brain complex (Figure 2D). Therefore, this construct was used for in vivo experiments. The PDZ13 domain of MUPP1 fused with the TAT peptide (TAT-PDZ13) also effectively and specifically disrupted the MUPP1-SynGAP interaction in the native complex (Figure 2E) and was used as a tool to disrupt the MUPP1-SynGAP interaction in living neurons. TAT-PDZ13 and TAT-SynGAP111 did not inhibit SynGAP-PSD-95 coimmunoprecipitation from rat brain lysates (see the Supplemental Data and Supplemental Figure S2). To insure that the functional changes that we evoked in living neurons by the application of cell-permeable peptides were the result of endogenous SynGAP-MUPP1 complex disruption, we always tested the effects of two unrelated SynGAP- and MUPP1-derived peptides together with their noncompeting peptide homologs. It seems unlikely that disruption of unrelated SynGAP interactions and unrelated MUPP1 interactions would coincidentally result in similar functional changes.

MUPP1-SynGAP Interactions Are Not Required for SynGAP Anchoring in the Synapse

As we showed in coimmunoprecipitation assays, TAT-PDZ13 disrupted MUPP1-SynGAP interactions, resulting in the dissociation of SynGAP from the native complex. We reasoned that this interaction could anchor SynGAP to the synapse, and we tested whether disruption of the MUPP1-SynGAP interaction affected SynGAP synaptic clustering in living neurons. Immunofluorescent staining of neurons confirmed that HA-tagged TAT fusion proteins penetrated cells within 10–15 min (data not shown). After 1 hr incubation with TAT proteins, cultured hippocampal neurons were fixed, and SynGAP immunofluorescent clusters were quantified with antibody specifically recognizing SynGAP-α. Since the average number of SynGAP clusters and the average intensity of fluorescence in the cluster were unchanged (Supplemental Figure S3 [http://www.neuron.org/cgi/content/full/43/4/563/DC1]), the MUPP1-SynGAP interaction does not appear to be critical for SynGAP synaptic localization. This suggests that, once localized, SynGAP is constrained in some fashion, perhaps by a protein other than MUPP1.

CaMKII-Dependent In Vivo SynGAP Phosphorylation

Chen et al. (1998) showed that SynGAP can be phosphorylated by CaMKII in vitro and hypothesized that Ca^{2+} entering the synapse through activated NMDARs would regulate SynGAP activity via CaMKII. Taking this data as a starting point, we examined SynGAP phosphorylation in vivo and tested whether its phosphorylation was dependent on the NMDAR and/or interactions with MUPP1. To monitor SynGAP phosphorylation in vivo, we metabolically labeled cultured hippocampal neurons with ^{32}P under conditions in which excitatory inputs were blocked (in the presence of 1 μM TTX, 5 μM nimodipine, 100 μM APV, and 40 μM CNQX). Labeled cells were lysed, SynGAP was immunoprecipitated, and the incorporation of ^{32}P into SynGAP was quantified. SynGAP immunoprecipitates revealed phosphorylated double bands that precisely matched the SynGAP Western blot images obtained from the same immunoprecipitates (Figure 3). The phosphorylated bands did not appear in immunoprecipitates using antibody preabsorbed

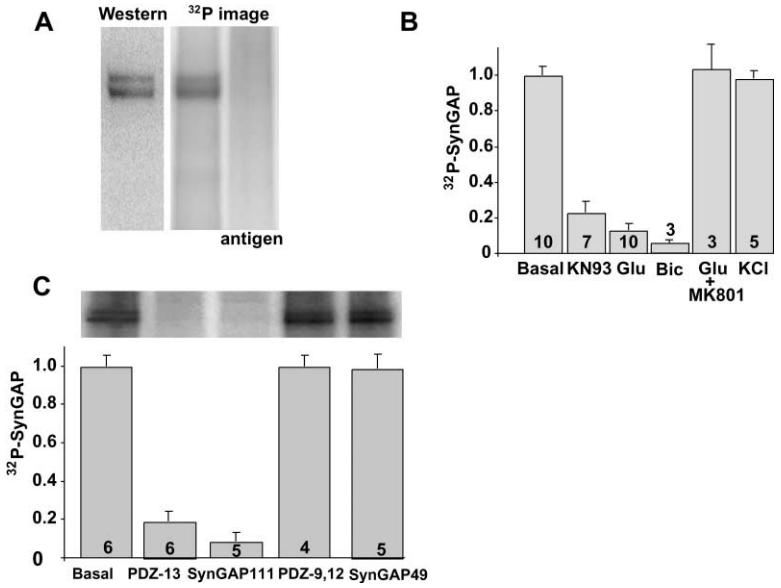

Figure 3. SynGAP Is Phosphorylated in Dormant Neurons in a CaMKII-Dependent Fashion and Dephosphorylated after NMDA Receptor Activation

(A) Image of in vivo phosphorylated SynGAP immunoprecipitated from ^{32}P metabolically labeled cultured hippocampal neurons (14 d.i.v.). The lane labeled "antigen" denotes the immunoprecipitate with αSynGAP preabsorbed by antigenic peptide.

(B) Comparison of in vivo SynGAP phosphorylation (mean ± SEM). KN93 (50 μM) and MK801 (10 μM) were added to the media 1 hr before cell lysis. Basal conditions refer to culture media containing TTX, APV, nimodipine, and CNQX (Experimental Procedures). Neurons were stimulated with 50 μM glutamate (Glu) or 10 μM bicuculline (Bic) 3 min before cell lysis. The numbers at the bottom of the bars designate the number of independent experiments.

(C) Cell-permeable MUPP1-PDZ13 and SynGAP111 induce SynGAP dephosphorylation. TAT-fusion peptides (5 μM) were included in the media 30 min before cell lysis.

with antigenic peptide. Thus, SynGAP is phosphorylated in cultured quiescent hippocampal neurons. Neuronal SynGAP phosphorylation was CaMKII dependent, since preexposure of neurons to the cell-permeable CaMKII inhibitor KN93 inhibited 80% of SynGAP phosphorylation (Figure 3B). The residual SynGAP phosphorylation could be the result of incomplete CaMKII inhibition or tyrosine phosphorylation (Pei et al., 2001).

NMDA Receptor Activation Dephosphorylates SynGAP in Living Neurons

Strikingly, SynGAP was *dephosphorylated* by ~90% after stimulation of neurons with 50 μM glutamate or stimulation of synaptic inputs by application of 10 μM bicuculline (3 min bath application; Figure 3B). The NMDAR channel blocker MK801 prevented glutamate-stimulated SynGAP dephosphorylation, indicating that Ca^{2+} entering neurons via the NMDA receptor initiated this dephosphorylation (Figure 3B). The specific requirement of NMDAR activity for SynGAP dephosphorylation was supported by the observation that depolarization-induced activation of voltage-dependent Ca^{2+} channels did not change the extent of SynGAP phosphorylation (Figure 3B).

In Vivo Disruption of the SynGAP-MUPP1 Complex also Dephosphorylates SynGAP

To disrupt the MUPP1-SynGAP complex in cultured rat hippocampal neurons, cells were incubated with TAT-PDZ13 or TAT-SynGAP111 in the presence of TTX/nimodipine/APV/MK801/CNQX inhibitors to prevent Ca^{2+} influx. Exposure of the neurons for 30 min to 5 μM of either peptide resulted in almost complete SynGAP dephosphorylation (Figure 3C). This effect appears to be specific, since noncompetitive, homologous TAT peptides (TAT-PDZ12, TAT-PDZ9, and TAT-SynGAP49) did not alter SynGAP phosphorylation.

CaMKII Directly Binds MUPP1

Dissociation of SynGAP from MUPP1 resulted in SynGAP dephosphorylation, suggesting that close contact with CaMKII was required for the maintenance of CaMKII-mediated SynGAP phosphorylation. We next asked if CaMKII was in the MUPP1 complex. αSynGAP and αMUPP1 coimmunoprecipitated CaMKII from solubilized rat brain synaptosomes (Figure 4A). In control experiments, antibody preabsorption with antigenic peptides blocked this coimmunoprecipitation, and SynGAP and MUPP1 antibody did not immunoprecipitate heterologously expressed CaMKII (data not shown). FLAG-tagged MUPP1 coimmunoprecipitated CaMKIIα and CaMKIIβ when coexpressed in 293T cells (Figure 4B). In vitro-translated MUPP1 coimmunoprecipitated in vitro-translated CaMKIIα, but a MUPP1 fragment containing PDZ domains 8–13 did not bind CaMKII (Supplemental Figure S4A [http://www.neuron.org/cgi/content/full/43/4/563/DC1]). Further investigation of this interaction with GST fusion peptides containing PDZ domains 1–7 (Supplemental Figure S4B) showed that CaMKII most strongly interacts with MUPP1-PDZ2 and more weakly with PDZ5, -6, and -7. Finally, purified brain CaMKII specifically bound the purified PDZ2 domain (Figure 4C), confirming that CaMKII and MUPP1 interact directly. To verify that CaMKII-MUPP1 is a bona fide PDZ interaction, we mutated the PDZ signature sequence GLGF, which is critical for the binding of PDZ ligands (Doyle et al., 1996). CaMKII did not bind the PDZ2 domain when GLGF was mutated to PSES (Supplemental Figure S4C).

Typically, PDZ domains bind proteins via a four amino acid motif located on their C terminus (Hung and Sheng, 2002), but no such canonical PDZ motif is present on the CaMKII C terminus. Nevertheless, the CaMKII C terminus must be necessary for binding, since a CaMKII protein truncated after amino acid 290 ("constitutively active" CaMKII) did not bind MUPP1 (data not shown). PDZ domains can also interact with internal peptide sequences, as demonstrated by the binding of neuronal nitric oxide synthase (nNOS) to the PDZ domain of PSD-95 or syntrophin. A two-stranded hairpin "finger" of nNOS, formed by two short β sheets, docks the groove of the syntrophin PDZ domain (Tochio et al., 1999). Alignment of CaMKII and nNOS sequences revealed a striking

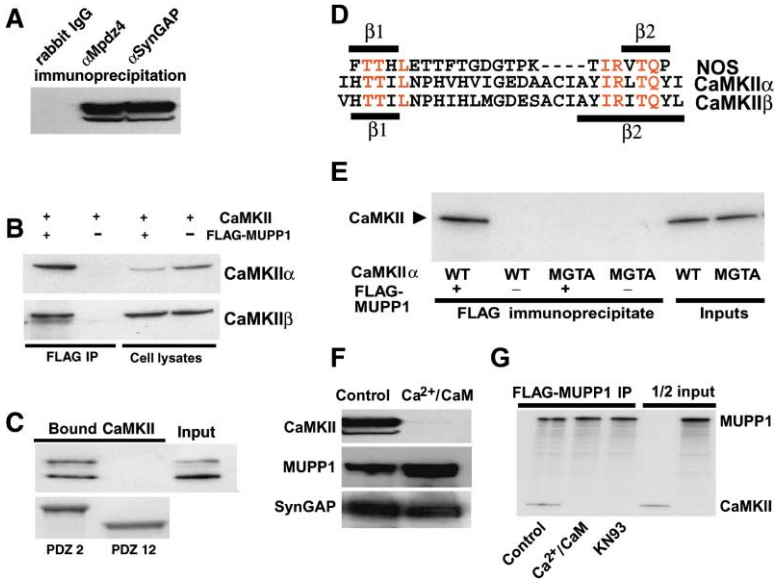

Figure 4. CaMKII Directly Binds MUPP1 and Ca^{2+}/CaM Prevents Binding

(A) αSynGAP and αMUPP1 coimmunoprecipitate CaMKII from solubilized rat brain synaptosomes. The two distinct bands seen on the Western blot likely represent CaMKIIα and CaMKIIβ recognized with monoclonal CaMKII antibody.

(B) MUPP1 binds CaMKIIα and CaMKIIβ heterologously expressed in mammalian cells. CaMKIIs were expressed with or without FLAG-MUPP1 in 293T cells. The cell lysate was immunoprecipitated with αFLAG and probed with αCaMKII.

(C) CaMKII directly binds the second PDZ domain of MUPP1. *E. coli* expressed and purified His-tagged MUPP1 PDZ2 and PDZ12 were mixed with purified bovine brain CaMKII (mixture of α and β isoforms) and precipitated using Ni beads (Western blot with CaMKII antibody).

(D) Alignment of nNOS and CaMKII sequences (containing two short C-terminal β strands predicted by MacVector software). The region between β structures contains amino acids 411–437 of rat CaMKIIα.

(E) CaMKIIα mutation of four amino acids eliminating the second predicted C-terminal β strand (amino acids 432–435, IRLT > MGTA) prevented MUPP1 binding. ^{35}S-labeled CaMKIIα and FLAG-MUPP1 were precipitated with FLAG antibody.

(F) Ca^{2+}/CaM dissociates CaMKII and SynGAP in the native complex. SynGAP was immunoprecipitated from solubilized P2 brain microsomes, with or without 25 μM CaM plus 0.5 mM $CaCl_2$, and the precipitate was probed with αCaMKII, αMpdz4, and αSynGAP on Western blot.

(G) Ca^{2+}/CaM prevents CaMKII binding to MUPP1. ^{35}S-labeled FLAG-MUPP1 and CaMKIIα were translated in vitro, incubated with or without 25 μM CaM plus 0.5 mM $CaCl_2$ or 50 μM KN93, and precipitated with αFLAG.

sequence similarity between the hairpin-forming β sheets of nNOS and the two short β sheets on the C terminus of CaMKII (Figure 4D). Replacing four amino acids in this region (CaMKIIα, amino acids 432–435, IRLT to MGTA) eliminated the second predicted β sheet and completely prevented the binding of CaMKII to MUPP1 (Figure 4E). This result suggested that, like nNOS, CaMKII binds its PDZ domain via an internal hairpin finger motif.

Ca^{2+}/CaM Binding Releases CaMKII from MUPP1

The experiments so far are most simply interpreted as MUPP1 holding SynGAP and CaMKII in proximity. We speculate that this scaffolding allows CaMKII to phosphorylate (directly or indirectly) bound SynGAP-α in neurons in which excitatory Ca^{2+} influx is blocked. Given that both the disruption of the SynGAP-MUPP1 link and Ca^{2+} influx via the NMDAR resulted in SynGAP dephosphorylation, Ca^{2+} might dissociate one of the molecules from MUPP1. To examine this hypothesis, we first tested the effect of Ca^{2+}/CaM on the SynGAP-CaMKII interaction in the native complex. Figure 4F shows that Ca^{2+}/CaM dissociated the SynGAP-CaMKII interaction, leaving SynGAP complexed to MUPP1. Since CaMKII binds Ca^{2+}/CaM, we tested whether Ca^{2+}/CaM binding dissociated CaMKII from MUPP1. In vitro assays demonstrated that Ca^{2+}/CaM-free but not Ca^{2+}/CaM-bound CaMKII interacted with MUPP1 (Figure 4G). Ca^{2+} alone did not dissociate CaMKII from MUPP1, and Ca^{2+}/CaM did not disrupt SynGAP's interaction with MUPP1 (data not shown). Interestingly, the competitive CaMKII inhibitor KN93 binds to the same site as Ca^{2+}/CaM and also dissociates CaMKII from MUPP1 (Figure 4G). These data suggest that simple occupation of a Ca^{2+}/CaM binding site but not transition of CaMKII into its active state is sufficient to prevent CaMKII-MUPP1 binding. Thus, MUPP1 approximates SynGAP to CaMKII, resulting in SynGAP phosphorylation. Ca^{2+} entering the synapse via the NMDAR binds CaMKII and dissociates it from the MUPP1-SynGAP complex. SynGAP is then dephosphorylated by an undetermined phosphatase.

Disruption of SynGAP-MUPP1 Interaction Results in p38 MAP Kinase Inactivation

Both NMDAR-mediated Ca^{2+} influx and disruption of the SynGAP-MUPP1 interaction resulted in SynGAP dephosphorylation. We reasoned that SynGAP-MUPP1 dissociating peptides could be used as SynGAP modulators that mimic NMDAR activation, but without affecting other NMDAR-activated targets. SynGAP regulates the activity of the Ras, and in turn Ras regulates ERK MAP kinase activity (Iida et al., 2001). We tested whether disruption of the SynGAP-MUPP1 interaction affected ERK activity. ERK1 and ERK2 activities in cultured hippocampal neurons were measured by immunofluorescent staining of neurons using antibodies that specifically recognized the active (phosphorylated) form of ERK. Neuron exposure for 30–60 min to TAT-PDZ13 or TAT-SynGAP111 (5 μM) did not change basal or bicuculline-stimulated ERK activity in pyramidal neurons (Figure 5A). Surprisingly, both blocking peptides significantly attenuated the phosphorylation (activity) of p38 MAPK (Figure 5B), decreasing it to the same level reached after synaptic stimulation.

This result implicates SynGAP in the regulation of p38

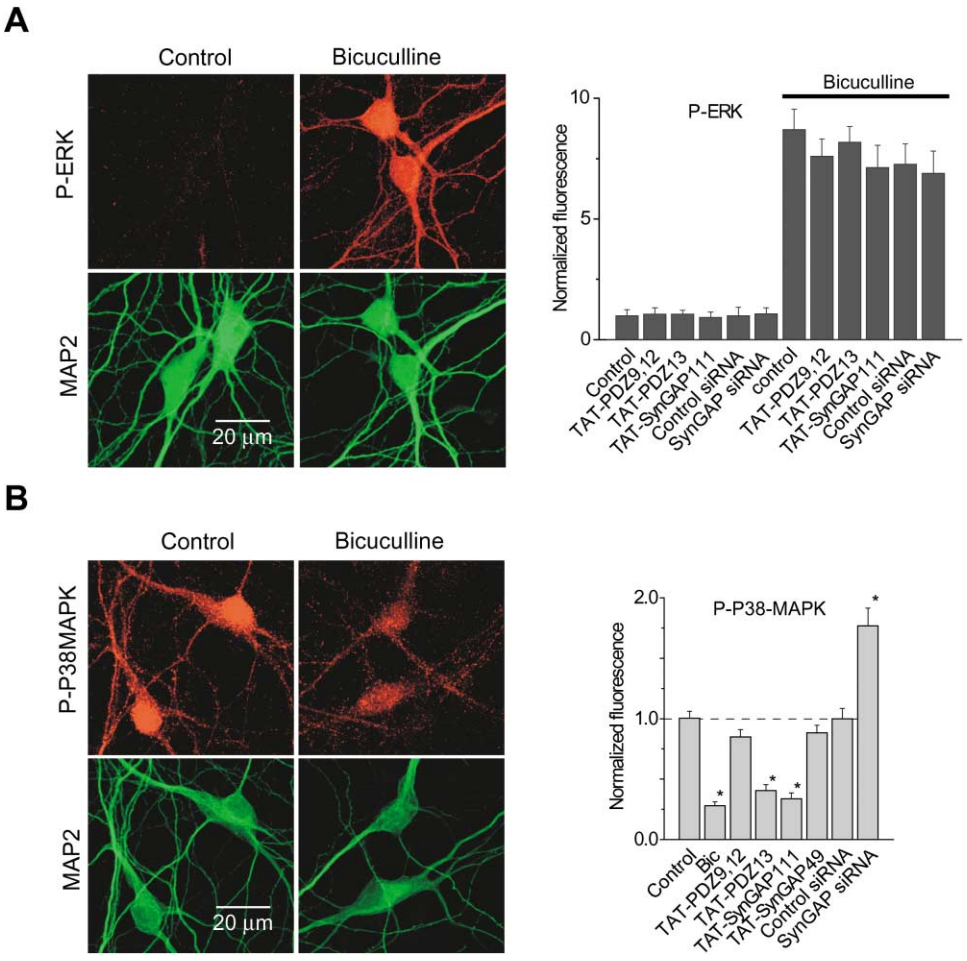

Figure 5. SynGAP Dissociation from the MUPP1-CaMKII Complex Does Not Affect ERK Activity and Attenuates the Activity of P38-MAPK

(A) Double immunofluorescence staining of 14 d.i.v. neurons with neuronal-specific Map2 antibody (bottom rows) and phospho-ERK antibody (upper row). Data are shown for control conditions (see Experimental Procedures) and after 5 min incubation with 10 μM bicuculline and 10 μM glycine. The bar graph illustrates the average effect of cell-permeable peptides (5 μM, 30 min, n = 6) and SynGAP-α siRNA (5–6 days posttransfection, n = 4) on ERK activity.

(B) Images and normalized fluorescence of neurons double stained with Map2 antibody (bottom rows) and phospho-p38 MAP Kinase antibody (upper row). Population data summarize the effect of cell-permeable peptides (5 μM, 30 min, n = 6) and SynGAP-α siRNA (5–6 days posttransfection, n = 4) on p38 MAPK activity. Asterisks indicate values significantly different from control $p < 0.01$ in both (A) and (B).

MAPK activity. To test this conclusion using an independent method, siRNA was targeted to a SynGAP-α-specific coding region (bases 3605–3623 of the AF058790 coding sequence). In cultured hippocampal neurons 5–6 days after transfection, the SynGAP protein level dropped to <10% of that in neurons transfected with nonsilencing RNA (Supplemental Figure S5 [http://www.neuron.org/cgi/content/full/43/4/563/DC1]). SynGAP knockdown resulted in a marked increase in p38MAPK activity without affecting ERK activity (Figure 5), verifying the role of SynGAP in the pathway governing p38 MAPK activity. Since SynGAP knockdown (equivalent to attenuation of SynGAP activity) augments p38 MAPK and SynGAP dissociation from MUPP1 decreases its activity, we conclude that dissociated and dephosphorylated SynGAP is more active than the phosphorylated SynGAP in the MUPP1-CaMKII complex.

SynGAP Predominantly Activates Rap GTPase Activity

P38 MAPK activity is regulated by multiple upstream signals including the small GTPases Rac, Ras, and Rap (Salojin et al., 1999; Palsson et al., 2000). In hippocampal neurons, p38 MAPK activity was regulated by Rap but not Ras activity (Zhu et al., 2002). Since earlier SynGAP activity was only tested with Ras (Chen et al., 1998), we compared SynGAP's effect on Ras and Rap GTPase activity using an in vitro assay. As shown on the Figures 6A and 6B, SynGAP stimulated Rap GTPase activity much more potently than Ras GTPase activity (2-fold maximum stimulation of Ras GTPase compared to a 10-fold stimulation of Rap GTPase). Moreover, Rap GTPase activity increased linearly with SynGAP concentration, whereas Ras GTPase activity scarcely changed over the same concentration range (Figure 6C). Both Rap1 and

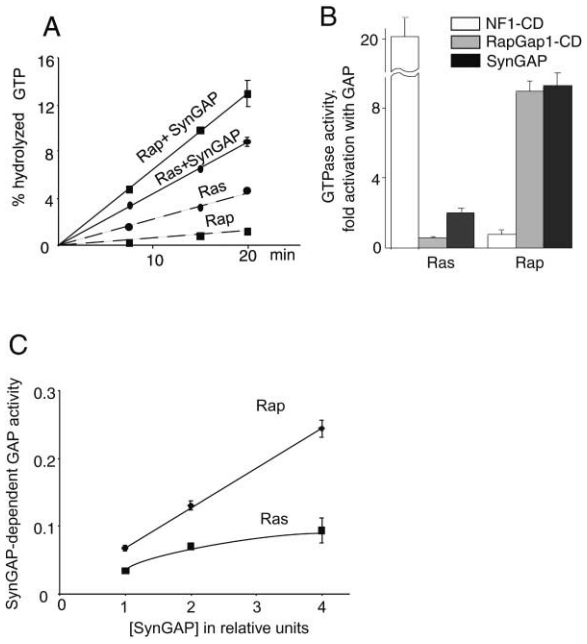

Figure 6. SynGAP Activates Rap GTPase In Vitro

(A) Kinetics of GTP hydrolysis by Ras and Rap stimulated with SynGAP.

(B) Comparison of RasGAP and RapGAP SynGAP activity. Activities of RasGAP NF1 catalytic domain (CD) and Rap1GAP-CD served as controls in parallel assays.

(C) SynGAP activity dose response curve. GAP activity is expressed as percent of hydrolyzed GTP/15 min minus values under control conditions.

Rap2 GTPases were similarly activated with SynGAP (data not shown). These data suggest that, in living cells, SynGAP predominantly activates Rap GTPase.

MUPP1-SynGAP Complex Disruption Increases the Frequency of AMPA mEPSCs and the Number of AMPAR Clusters

Experiments with *SynGAP*$^{-/-}$ mice implicate SynGAP in the regulation of LTP and synaptic AMPARs (Komiyama et al., 2002; Kim et al., 2003). Rap-dependent p38 MAPK activity also affected AMPA receptor synaptic trafficking and LTD (Zhu et al., 2002). We examined whether the MUPP1-SynGAP interaction affected synaptic AMPAR activity. To avoid possible complications related to Ca^{2+} influx, all experiments were performed under conditions suppressing most channels other than the AMPAR (Experimental Procedures). The inclusion of the cell-impermeable binding domain blocking peptides PDZ13 or SynGAP111 into the patch pipette induced a significant increase in both AMPA mEPSCs frequency and amplitude (Figure 7A). The homologous control peptides PDZ9, PDZ12, or SynGAP49 did not change AMPA mEPSCs. The potentiation lasted for the duration of the recordings (30–40 min) and correlated with a progressive increase in the amplitude of responses induced by application of AMPA to the soma and proximal dendrites (Figure 7B). Taken together, these observations strongly suggest that dissociation of SynGAP from MUPP1 potentiates the AMPAR response in postsynaptic neurons. Similar results were obtained using TAT-fused peptides in the pipette (data not shown). Since all biochemical experiments were carried out with extracellular application of the membrane-permeant TAT peptides, we also tested these peptides on AMPA mEPSCs. The extracellular application of TAT-PDZ13 and TAT-SynGAP111 peptides also induced a relatively rapid (4–5 min) and long-lasting increase in the frequency and amplitude of AMPAR-mediated mEPSCs (data not shown). Potentiation of the AMPA response could be related to changes in the AMPAR phosphorylation state or membrane targeting (Gomes et al., 2003). Therefore, we used immunofluorescent labeling to determine if disruption of the MUPP1-SynGAP interaction modified the number of GluR synaptic clusters.

Cultured hippocampal neurons exposed to TAT-PDZ13 or TAT-SynGAP111 showed a significant increase in the number of GluR1- and GluR2,3-positive clusters as compared to control untreated neurons and neurons incubated with TAT-PDZ12 or TAT-SynGAP49 (Figure 7C). The number of NR1 clusters did not increase significantly during these experiments (Figure 7C), indicating that the total number of excitatory synapses was not changed. These results demonstrate that disruption of the SynGAP-MUPP1 interaction results in an increase in the number of postsynaptic AMPARs and support the hypothesis that SynGAP is involved in the regulation of AMPAR synaptic targeting. To test this hypothesis using an independent method, we measured the number of GluR1- and GluR2,3-positive clusters in hippocampal neurons in which SynGAP-α was decreased using SynGAP-specific siRNA. Figure 7C demonstrates that SynGAP knockdown significantly decreased the number of GluR1 and GluR2,3 synaptic clusters.

Discussion

We investigated the role of the GTPase-activating protein SynGAP in the signal transduction cascade between NMDARs and AMPARs in live hippocampal neuron synapses. We demonstrated that, in the synaptic NMDAR complex of hippocampal neurons, SynGAP-α and CaMKII are coupled via direct binding to PDZ domains of the multi-PDZ domain protein MUPP1. CaMKII binds MUPP1 only in its Ca^{2+}-free state. In the dormant neuron, SynGAP phosphorylation requires CaMKII activity. Upon activation of NMDARs, Ca^{2+} enters the synapse and drives SynGAP dephosphorylation. These results suggest that the NMDA-mediated increase in local [Ca^{2+}] causes dissociation of CaMKII from the SynGAP-MUPP1 complex, which decreases SynGAP phosphorylation (Figure 8).

While this manuscript was under review, Oh et al. (2004) reported that direct SynGAP phosphorylation with CaMKII resulted in a moderate increase of SynGAP activity and stimulation of cultured neurons with NMDA resulted in an increase of SynGAP serine 765 and 1123 phosphorylation. There are several potential explanations for this apparent contradiction with our SynGAP phosphorylation data. First, the phosphorylation that we observed in live hippocampal neurons might not be the

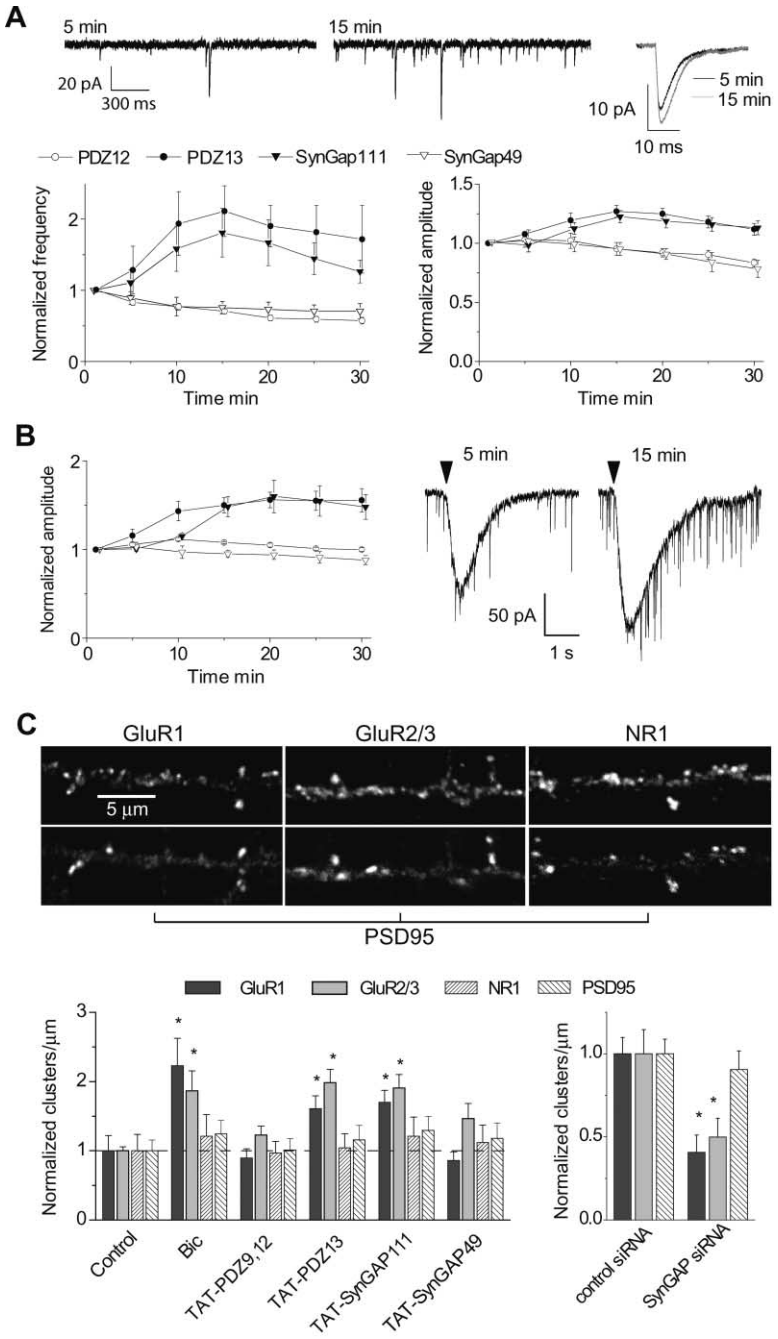

Figure 7. Increased AMPARs in Cultured Hippocampal Neurons after Disruption of the MUPP1-SynGAP Interaction

(A) Potentiation of miniature AMPA EPSCs. The traces are examples of mEPSCs recorded from hippocampal neurons in culture with the patch pipette containing 5 μM PDZ13 peptide. Right plot illustrates averaged traces of EPSCs after analysis of 500 consecutive events, monitored 5 and 15 min after the beginning of patch recording. Lower plots show the averaged amplitude and frequency of mEPSCs recorded in the presence of peptides in the patch pipette (n = 4). Data were normalized to the mean values obtained during the first 2 min of patch clamp recording.

(B) AMPAR responses induced by short (100 ms) local application of AMPA to the soma of the neuron (n = 4). Traces illustrate responses obtained between 5 and 15 min of patch clamp recording from a neuron filled with 5 μM PDZ13 peptide. Triangles indicate the time of agonist application. Plots display averaged (n = 4) data. All values shown in (A) and (B) that were obtained with peptides PDZ13 and SynGAP111 after 15 min of recording are significantly different from those obtained with PDZ12 and SynGAP49.

(C) Disruption of the MUPP1-SynGAP interaction increased and siRNA-mediated SynGAP knockdown decreased the number of AMPAR clusters in cultured hippocampal neurons. (Top panel) Images of GluR, NR1, and PSD-95 clusters in 16 d.i.v. hippocampal neurons. (Lower panel) Effect of cell-permeable fragments of MUPP1 and SynGAP (5 μM, 30 min exposure, n = 4) and SynGAP-α siRNA (5–6 days posttransfection, n = 3) on the number of GluR1, GluR2/3, PSD-95, and NR1 clusters. "Bic" designates neurons stimulated with bicuculline. Asterisks indicate values significantly different from control $p < 0.05$.

result of direct CaMKII phosphorylation, but may be mediated by an unidentified CaMKII-dependent kinase bound to the same MUPP1 complex (e.g., the Unc51.1 kinase that was recently proposed to directly interact with SynGAP [Tomoda et al., 2004]). Second, Oh et al. may have detected hyperphosphorylation of SynGAP-β that is directly bound to CaMKII (Li et al., 2001), while our data describe the behavior of SynGAP-α. Finally, the experimental conditions in the two sets of experiments are quite different; we stimulated neurons with glutamate and bicuculline (versus NMDA) for 3 min (versus 15 s) and measured total ^{32}P incorporation (versus specific serine phosphorylation). Oh et al. used cultures of mice cortical neurons, whereas we studied primary cultures of rat hippocampal neurons. Further experiments are needed to resolve these differences.

The binding of SynGAP to MUPP1 is critical for SynGAP phosphorylation and the regulation of downstream pathways. Disruption of this complex with specific peptides resulted in SynGAP dephosphorylation, inactivation of P38 MAPK, and an increase in the number of synapses containing functional AMPARs. SynGAP's regulation of p38 MAPK activity and AMPAR subunit targeting to synapses were confirmed by our experiments with siRNA-mediated SynGAP-α knockdown. Together with our finding that SynGAP more potently ac-

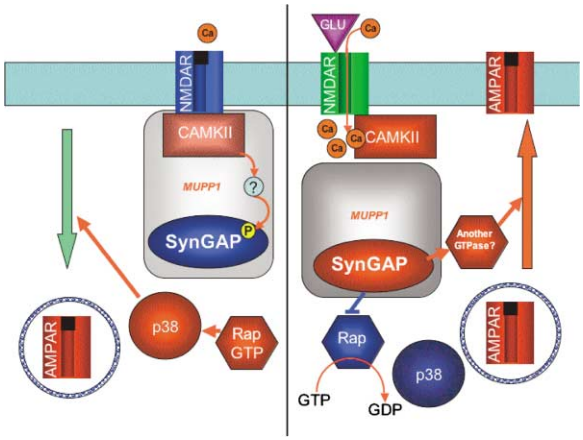

Figure 8. Model of NMDAR-Regulated SynGAP Activity

See the text for details.

tivates Rap than Ras, these results suggest a model (Figure 8) in which NMDAR-and CaMKII-dependent SynGAP dephosphorylation increases its GAP activity, inactivates Rap, and thus attenuates p38 MAPK activity. The result of p38 MAPK inactivation is increased incorporation of functional AMPA receptors into the synapse.

There are several surprising results from these studies. First, it is counterintuitive that SynGAP is phosphorylated in a CaMKII-dependent fashion in dormant neurons where intracellular [Ca^{2+}] is low. We showed that SynGAP is potently dephosphorylated when CaMKII was inhibited by KN93. Thus, CaMKII complexed with MUPP1 and SynGAP is active in synapses of dormant neurons. This conclusion does not agree with the generally accepted mechanism of CaMKII activation *after* Ca^{2+} entry (reviewed in Lisman et al., 2002). However, recent findings revealed that CaMKII binding to the NMDAR NR2B subunit can lock the kinase in its active state (Bayer et al., 2001). It is possible that a fraction of active CaMKII bound to MUPP1 and NMDAR or another yet unknown molecule allows SynGAP phosphorylation even in the absence of tonic activity.

Another unusual finding of this study is that direct interaction of CaMKII with the PDZ domains of MUPP1 occurs via a noncanonical internal sequence. The striking similarity between CaMKII and NOS sequences of β strands flanking the "finger" suggests that the CaMKII PDZ binding domain (amino acids 411–437 of the rat CaMKII-α sequence) is similar to the "β finger" PDZ binding domain of NOS (Tochio et al., 1999). A hairpin formed by the two flanking β strands is absolutely essential to NOS-PDZ binding, and the amino acids that are crucial to the structural integrity of the hairpin are as important, or are more important than, residues that make direct contacts (Harris et al., 2001). In support of the proposed similarity between the NOS and CaMKII PDZ binding domains, point mutations eliminating the second β strand prevented CaMKII from binding to MUPP1. Given the importance of CaMKII in synaptic function and the abundance of PDZ domain-containing proteins in synapses (Sheng and Sala, 2001), this type of interaction may be important for regulated kinase targeting to synaptic supramolecular complexes.

The third surprising finding is that SynGAP, despite its closer homology to RasGAPs, is a much better GAP for Rap than Ras. This is supported by our direct in vitro measurements of SynGAP regulation of Rap and Ras GTPase activity. This dual Ras/RapGAP activity is not unique for SynGAP. The RasGAP-related protein GAP^{IP4BP} has been reported to stimulate the GTPase activity of both Ras and Rap1 (Cullen et al., 1995). In line with these observations, Bud2 from *Saccharomyces cerevisiae* is homologous to the RasGAP domain but acts on Bud1p/Rsr1p, a putative yeast homolog of Rap1 (Park et al., 1993).

The finding of SynGAP RapGAP activity is especially important to the model of Figure 8. We demonstrated that either NMDAR-mediated Ca^{2+} influx or disruption of the SynGAP-MUPP1 complex resulted in SynGAP dephosphorylation. We hypothesize that dissociation of the SynGAP-MUPP1 complex with specific peptides mimics NMDAR-dependent SynGAP regulation without affecting other NMDAR-activated pathways. If this hypothesis is correct, then dephosphorylation activates SynGAP, which in turn inactivates Rap. Our finding further supports the suggestion that SynGAP knockdown (equivalent to activity attenuation) increased p38 MAPK activity, while SynGAP dephosphorylation had the opposite effect. Inactivated Rap no longer drives p38 MAPK, and as a result, AMPARs are no longer being actively removed from the synapse. This model is consistent with the results of Zhu et al. (2002), who demonstrated that p38 MAP kinase is activated by Rap, not Ras, and that Rap-dependent p38 MAPK activity promotes the removal of AMPAR subunits from synapses. However, this model does not agree with the slight increase in AMPAR number found in cultured neurons from *SynGAP*$^{-/-}$ mice (Kim et al., 2003). The latter may be a developmental effect, since siRNA-mediated SynGAP-α knockdown in cultured hippocampal neurons results in a significant decrease of both GluR1 and GluR2,3 subunit synaptic clusters.

All of the results described in this paper are related to one of the SynGAP isoforms, SynGAP-α. The fact that both isoforms directly (Li et al., 2001) or indirectly (via MUPP1; data presented here) bind CaMKII emphasizes the importance of SynGAP-CaMKII proximity. The existence of two separate SynGAP-CaMKII complexes suggests that the two SynGAP isoforms may regulate separate pathways.

Our immunofluorescent study demonstrated that SynGAP-MUPP1 disruption increased the number of GluR1 clusters, suggesting that SynGAP activity affects trafficking of the AMPAR GluR1 subunit. GluR1 trafficking depends on Ras-regulated ERK MAPK (Zhu et al., 2002). Since SynGAP/MUPP1 dissociation and siRNA-mediated SynGAP-α knockdown did not change ERK activity, SynGAP-α may affect other pathways regulating the number of AMPARs in synapses (e.g., PI3K pathway [Man et al., 2003]).

In summary, the SynGAP-α-MUPP1-CAMKII complex is a component of the NMDAR supramolecular structure in hippocampal pyramidal neurons. The integrity of this complex is critical for synaptic NMDAR-dependent AMPA receptor trafficking.

Experimental Procedures

Yeast Two-Hybrid Screening

Sequences encoding the PDZ domains of MUPP1 were selected using the Swiss Institute for Experimental Cancer Research (ISREC) ProfileScan software. cDNAs encoding each of the 13 PDZ domains of human MUPP1 were subcloned into the Gal 4 binding domain fusion vector pGBKT7 (BD-Clontech). These constructs were used for screening the human brain library (Matchmaker pACT2, Clontech) expressed in AH109 yeast. The PDZ13 bait contained bases 5917–6213 (amino acids 1973–2071) of human MUPP1 (accession number NP_003820).

cDNA Constructs and Recombinant Proteins

Human MUPP1 PDZ domain sequences were subcloned into pET42.1 (Novagen) and expressed in BL21TrxLysS (Novagen) bacteria. GST fusion constructs of H-Ras and human Rap1A, Rap1B, Rap2A, and Rap2B were made by subcloning the coding sequences (obtained from Guthrie cDNA Resource Center) into pGEX4T (Amersham Bioscience) and were expressed in BL21 CodonPlus bacteria (Stratagene). GST fusion proteins were affinity purified on a glutathione resin (Amersham Bioscience).

His-HA-tagged TAT fusion constructs were made by subcloning the corresponding PCR fragments in-frame with the 6His-HA-TAT sequence into a HA-TAT vector (gift of Steven Dowdy, HHMI, UCSD). Fusion peptides were expressed in BL21TrxLysS bacteria (Novagen) and solubilized in buffer A (6 M urea/20 mM HEPES [pH 8.0]/100 mM NaCl). Cellular lysates were loaded onto a 2 ml Ni-NTA column (Qiagen) in buffer A plus 10 mM imidazole, washed, and eluted with 0.2 M imidazole in buffer A. Proteins were bound to HiTrapQ or HiTrapSP (TAT-PDZ9) 1 ml resin (Amersham Bioscience), washed with urea-free buffer, and eluted with Buffer B (0.5 M Na carbonate, 1 M NaCl [pH 11]). Finally, proteins were desalted on a HiTrap desalting column (5 ml, Amersham Bioscience) equilibrated with Buffer C (50 mM Na-HEPES, 100 mM NaCl, 10% Glycerol [pH 7.6]). Protein stock concentrations were 200–500 μM. 6xHis-HA-peptide constructs without TAT were made by excision of the TAT-encoding sequences from the constructs and the proteins were expressed and purified as described above.

For in vitro translation and mammalian cell expression, coding sequences or fragments of human MUPP1 (made by PCR) and rat SynGAP-α (gift of Richard Huganir, HHMI, Johns Hopkins) were subcloned in-frame in a modified pcDNA6 vector containing the N-terminal fusion for an HA- or FLAG-tag sequence. Coding sequences of rat CAMKIIα and -β, rat PSD-95, and rat CaMKII were subcloned into pcDNA3.1. Purified bovine brain CaMKII was purchased from Upstate Biotechnology (Lake Placid, NY).

^{35}S-labeled proteins were made with the T7-TNT system (Invitrogen) and [^{35}S]-methionine according to the manufacturer's protocol. For nonlabeled proteins, [^{35}S]-methionine was substituted with 1 mM unlabeled methionine.

Cell Cultures and Transfections

HEK293T cells were grown in DMEM/F12 media supplemented with glycine, Na-hypoxanthine, penicillin/streptomycin, and 10% FBS. Cells were transfected using Lipofectamine 2000 (Invitrogen) and cultured for 48 hr. Neurons from 18-day-old rat embryos were dissociated in trypsin and plated on coverslips coated with poly-L-lysine in minimal essential medium (MEM) with 10% NU serum (BD Biosciences) at densities of 30,000 cells/cm^2 (Brewer, 1995). On days 7 and 11 of growth in vitro (d.i.v.), half the medium was changed to MEM with 2% B27 supplement (Invitrogen). For biochemical experiments, neurons were grown for 14 days in 10 cm dishes covered with poly-L-lysine at a density of 4–6 $\times$ 10^6 cells per dish.

siRNA was designed and produced by Ambion to a unique region of SynGAP-α not present in the SynGAP-β sequence (bases 3605–3623 of AF058790 coding sequence). Double stranded siRNA (200 nM) was transfected into 11 d.i.v. neurons using Lipofectamine 2000. Nonsilencing double stranded RNA (Ambion) was used as a negative control. The relative amount of SynGAP in transfected neurons was quantified by WB of cell lysates using a chemiluminescent imager LAS-1000 (Fujifilm). All values were normalized to PSD-95 content.

Antibody, Immunoprecipitation, and Pull-Down Assays

Rabbit MUPP1 antibodies were made against GST fusions containing amino acids 460–535 (αMpdz2) or 1715–2040 (αMpdz4) of human MUPP1 and were affinity purified. Both antibodies recognized Flag-MUPP1 expressed in HEK293T cells (Western blot) and immunoprecipitated it. αMpdz4 was specific for immunofluorescent (IF) recognition of FLAG-MUPP1 expressed in COS-7 cells (data not shown). Rabbit SynGAP antibody (Upstate Biotechnology) was used for SynGAP Western blot (WB), immunoprecipitation (IP), and IF. This antibody was made to the last 20 amino acids of the SynGAP-α splice variant and did not recognize SynGAP-β. We used mouse monoclonal PSD-95 antibody (Upstate Biotechnology) for WB and IF, mouse monoclonal CaMKIIα and -β (BD transduction Laboratories), mouse NR1 antibody (C-terminal, Upstate Biotechnology) for WB, rabbit polyclonal NR1 antibody (AB1516, Chemicon) for IF, rabbit polyclonal GluR1 (Chemicon) and GluR2,3 (Upstate Biotechnology), rabbit polyclonal phospho-ERK1 and -2 and phospho-p38 MAPK (Cell Signaling Technology, Beverly, MA), mouse monoclonal MAP2 antibody (Sigma), mouse monoclonal M2-FLAG antibody (Sigma), and mouse monoclonal HA antibody (Santa Cruz).

For pull-down assays, 5 μl of in vitro-translated SynGAP was incubated for 1 hr at 4°C with 1 μg of GST-PDZ9, -12, or -13 bound to glutathione beads in 300 μl RIPA buffer (20 mM Tris-Cl [pH 8.0], 150 mM NaCl, 1% Triton X-100, 0.5% Na-Cholate, 0.1% SDS), washed with RIPA buffer, and solubilized in SDS sample buffer. For in vitro binding assays, 5–10 μl of in vitro-translated molecules were combined and incubated at 30°C for 30 min. The reaction was diluted in 300 μl RIPA, immunoprecipitated with the appropriate antibody, and the precipitate was washed with RIPA buffer.

Transfected cells were solubilized in lysis buffer (50 mM Tris-Cl [pH 8.0], 150 mM NaCl, 1% Triton X-100) supplemented with protease inhibitor cocktail (PIC, Roche), immunoprecipitated with the indicated antibody, and washed with lysis buffer.

Six- to eight-week-old rat brain P2 microsomes, synaptosomes, and PSD were isolated according to published procedures (Carlin et al., 1980) and solubilized in alkaline 1% sodium desoxycholate followed by dilution in 1% Triton X-100 as described (Luo et al., 1997). Solubilized protein (80 μg) was immunoprecipitated and probed on Western blot with the indicated antibodies. For all antibodies used in the immunoprecipitation experiments, negative controls were verified by antigen preabsorption. Also, all immunoprecipitating antibodies were tested for cross-reactivity with in vitro-translated coimmunoprecipitated molecules. Both control tests confirmed antibody specificity in immunoprecipitation assays and the absence of cross-reactivity of immunoprecipitating antibody.

Immunocytochemistry and Confocal Microscopy of Cultured Hippocampal Neurons

Three hours before all immunocytochemical experiments, 1 μM tetrodotoxin (TTX), 40 μM 6-cyano-7-nitroquinoxaline-2, 3-dione (CNQX), 100 μM 2-amino-5-phosphonovalerate (APV), and 5 μM nimodipine were added to neurons unless otherwise specified. Peptides (5 μM) were presented in culture media supplemented with the same inhibitors. To stimulate neurons with bicuculline, the media was replaced with one containing the following: 10 μM bicuculline and 10 μM glycine, 5 μM nimodipine (no TTX, CNQX, and APV added). After incubation with peptides (30 min) or stimulation with bicuculline (3–5 min) neurons were fixed with 4% formaldehyde, permeabilized with 0.2% Triton X-100, and blocked by 10% goat serum in PBS. Labeling was performed with mouse monoclonal PSD-95 antibody and one of the following rabbit antibodies: GluR1, GluR2/3, NR1, or SynGAP. Cy3-conjugated goat anti-rabbit IgG (Jackson ImmunoResearch Laboratories, Inc. West Grove, PA) and Alexa 488-conjugated goat anti-mouse IgG (Molecular Probes) were used as secondary antibodies. Images were acquired with an Olympus Fluoview-500 confocal microscope (60×, 1.4 objective, zoom 4). To quantify the distribution of clusters of neurons, we first focused on dendrites of neurons imaged with the fluorescent channel restricted to the PSD-95 label. Fluorescent images of GluR1, Glur2/3, or NR1 were then acquired. Cluster number and brightness were analyzed with the MetaMorph Imaging System (Universal Imaging, Westchester, PA). Ten neurons were analyzed from each experiment (three to four dendritic regions for each neuron). ERK1, ERK2, and

p38 MAPK activity in cultured hippocampal neurons was measured by immunofluorescent staining of neurons using antibodies that specifically recognized the active (phosphorylated) forms of ERK and p38 MAPK as described (Krapivinsky et al., 2003).

SynGAP In Vivo Phosphorylation Assay

Culture media was replaced with prewarmed, O_2/CO_2-saturated phosphorylation media containing phosphate-free MEM (ICN) supplemented with glutamine, pyruvate, and HEPES. This media also contained TTX (1 μM), CNQX (40 μM), APV (100 μM), MK801 (10 μM), and nimodipine (5 μM), unless otherwise specified. After 1 hr, the culture media was replaced by the same media but containing ^{32}P-orthophosphate, (2 mCi/ml, 6000 Ci/mmol, Perkin Elmer), and neurons were metabolically labeled for 1 hr. Neurons were stimulated for 3 min before lysis with 50 μM glutamate; 10 μM bicuculline, plus 10 μM glycine; or with 65 mM KCl (Tyrode's solution containing 75 mM NaCl, 65 mM KCl, 2 mM $CaCl_2$, 1 mM $MgCl_2$, 25 mM Na-HEPES, 10 mM Glucose, 0.1% BSA) at room temperature. For glutamate stimulation, media was replaced with one not containing CNQX, APV, and MK801 (and TTX for bicuculline stimulation) or CNQX and nimodipine for KCl stimulation. Neurons were then lysed in 1.5 ml of ice-cold lysis buffer containing 20 mM Na-HEPES (pH 7.5), 50 mM NaF, 10 mM K-pyrophosphate, 40 mM β-glycerophosphate, 10 mM EDTA, 0.1 μM okadaic acid, 0.5% Triton X-100, and PIC). Cells were scraped and centrifuged at 18,000 × g for 15m at 4°C. The pellet was resuspended in 50 mM Tris (pH 8.5), 2% SDS-200 mM DTT, and boiled for 10 min. Solubilized proteins were diluted 10-fold with the lysis buffer containing 1% Triton X-100 and 150 mM NaCl, and SynGAP was immunoprecipitated with SynGAP-α antibody. After electrophoresis, ^{32}P incorporation into SynGAP was quantified using Phosphorimager Storm 860 (Molecular Dynamics).

In Vitro GAP Assay

HEK293T cells were transfected with expression construct containing the HA-tagged NF1 catalytic domain (Xu et al., 1990), Rap1GAP catalytic domain (Brinkmann et al., 2002), or full-length SynGAP cDNA in pcDNA6 vector. Ras-specific NF1 and Rap-specific Rap1GAP activities were used as controls. Transfected cells were lysed 48 hr after transfection in a buffer containing 20 mM Tris (pH 8.0), 100 mM NaCl, 1% NP40, 1 mM DTT, and PIC, followed by immunoprecipitation with HA antibody. Precipitates were washed four times in lysis buffer and two times in GAP assay buffer (20 mM Tris [pH 7.4], 100 mM NaCl, 10 mM $MgCl_2$, 1 mM DTT, and 40 μg/ml BSA). Purified GST-H-Ras and GST-Rap GTPases (0.2 μM final concentration) were loaded with GTP (0.2 μM [γ-^{33}P]-GTP (6000 Ci/mmol, Perkin Elmer) for 15 min at 30°C in binding buffer (BB) (50 mM Tris [pH 7.5], 2 mM EDTA, 100 mM NaCl, 0.1 mM DTT, 0.5 mg/ml BSA, and 0.005% desoxycholate). Unbound GTP was separated from GTP bound GTPases using a microspin column (Autoseq50, Amersham Biotech), equilibrated with BB. Reactions were performed at 25°C in a 100 μl reaction containing 1 nM GTP bound GTPases and HA-GAP beads in GAP buffer with continuous mixing to maintain HA-GAP beads in suspension. The reaction was quenched with perchloric acid (5% final concentration; T = 4°C), and the inorganic ^{33}P was measured as described (Cowan et al., 2000).

Electrophysiological Recordings

Neurons (12–15 d.i.v.) were continuously perfused with an extracellular solution containing 140 mM NaCl, 2.5 mM KCl, 20 mM HEPES, 20 mM D-glucose, 2.0 mM $CaCl_2$, 2.0 mM $MgCl_2$, 0.01 mM bicuculline, 0.005 mM nimodipine, and 0.001 mM tetrodotoxin (pH 7.4). AMPA (100μM) dissolved in extracellular solution was pressure applied (Picospritzer) via a patch pipette placed 5–10 μm from the soma. TAT-conjugated peptides were perfused onto neurons via the recording chamber. Recording electrodes (4-6 MΩ) were pulled from borosilicate glass (TW150F-15; World Precision Instruments) and filled with solution containing 115 mM Cs methanesulfonate, 20 mM CsCl, 10 mM HEPES, 2.5 mM $MgCl_2$, 4 mM Na_2-ATP (adenosine triphosphate), 0.4 mM Na-GTP (guanosine triphosphate), 10 mM Na-phosphocreatine, and 0.6 mM EGTA (pH 7.2). Recordings were made using the Axopatch-200A amplifier and pCLAMP acquisition software (Axon Instruments). Series resistances (6–10 MΩ) were compensated. Data were low-pass filtered at 2 kHz and acquired at 10 kHz. AMPA receptor-mediated EPSCs were analyzed with MiniAnalysis software (Synaptosoft, Inc. Decatur, GA).

Statistical Analysis

All population data were expressed as the mean ± SEM. The Student's t test was employed to examine the statistical significance of the differences between groups of data.

Acknowledgments

We thank N. Otmakhov for stimulating discussions and helpful suggestions; and we thank Y. Manasian and C. Pellegrino for technical assistance.

Received: January 29, 2004
Revised: June 1, 2004
Accepted: July 28, 2004
Published: August 18, 2004

References

Bayer, K.U., De Koninck, P., Leonard, A.S., Hell, J.W., and Schulman, H. (2001). Interaction with the NMDA receptor locks CaMKII in an active conformation. Nature *411*, 801–805.

Brewer, G.J. (1995). Serum-free B27/neurobasal medium supports differentiated growth of neurons from the striatum, substantia nigra, septum, cerebral cortex, cerebellum, and dentate gyrus. J. Neurosci. Res. *42*, 674–683.

Brinkmann, T., Daumke, O., Herbrand, U., Kuhlmann, D., Stege, P., Ahmadian, M.R., and Wittinghofer, A. (2002). Rap-specific GTPase activating protein follows an alternative mechanism. J. Biol. Chem. *277*, 12525–12531.

Carlin, R.K., Grab, D.J., Cohen, R.S., and Siekevitz, P. (1980). Isolation and characterization of postsynaptic densities from various brain regions: enrichment of different types of postsynaptic densities. J. Cell Biol. *86*, 831–845.

Chen, H.J., Rojas-Soto, M., Oguni, A., and Kennedy, M.B. (1998). A synaptic Ras-GTPase activating protein (p135 SynGAP) inhibited by CaM kinase II. Neuron *20*, 895–904.

Cowan, C.W., Wensel, T.G., and Arshavsky, V.Y. (2000). Enzymology of GTPase acceleration in phototransduction. Methods Enzymol. *315*, 524–538.

Cullen, P.J., Hsuan, J.J., Truong, O., Letcher, A.J., Jackson, T.R., Dawson, A.P., and Irvine, R.F. (1995). Identification of a specific Ins(1,3,4,5)P4-binding protein as a member of the GAP1 family. Nature *376*, 527–530.

Doyle, D.A., Lee, A., Lewis, J., Kim, E., Sheng, M., and MacKinnon, R. (1996). Crystal structures of a complexed and peptide-free membrane protein-binding domain: molecular basis of peptide recognition by PDZ. Cell *85*, 1067–1076.

Gomes, A.R., Correia, S.S., Carvalho, A.L., and Duarte, C.B. (2003). Regulation of AMPA receptor activity, synaptic targeting and recycling: role in synaptic plasticity. Neurochem. Res. *28*, 1459–1473.

Harris, B.Z., Hillier, B.J., and Lim, W.A. (2001). Energetic determinants of internal motif recognition by PDZ domains. Biochemistry *40*, 5921–5930.

Hayashi, Y., Shi, S.H., Esteban, J.A., Piccini, A., Poncer, J.C., and Malinow, R. (2000). Driving AMPA receptors into synapses by LTP and CaMKII: requirement for GluR1 and PDZ domain interaction. Science *287*, 2262–2267.

Hung, A.Y., and Sheng, M. (2002). PDZ domains: structural modules for protein complex assembly. J. Biol. Chem. *277*, 5699–5702.

Husi, H., Ward, M.A., Choudhary, J.S., Blackstock, W.P., and Grant, S.G. (2000). Proteomic analysis of NMDA receptor-adhesion protein signaling complexes. Nat. Neurosci. *3*, 661–669.

Iida, N., Namikawa, K., Kiyama, H., Ueno, H., Nakamura, S., and Hattori, S. (2001). Requirement of Ras for the activation of mitogen-activated protein kinase by calcium influx, cAMP, and neurotrophin in hippocampal neurons. J. Neurosci. *21*, 6459–6466.

Kim, J.H., Liao, D., Lau, L.F., and Huganir, R.L. (1998). SynGAP: a

synaptic RasGAP that associates with the PSD-95/SAP90 protein family. Neuron *20*, 683–691.

Kim, J.H., Lee, H.K., Takamiya, K., and Huganir, R.L. (2003). The role of synaptic GTPase-activating protein in neuronal development and synaptic plasticity. J. Neurosci. *23*, 1119–1124.

Kimber, W.A., Trinkle-Mulcahy, L., Cheung, P.C., Deak, M., Marsden, L.J., Kieloch, A., Watt, S., Javier, R.T., Gray, A., Downes, C.P., et al. (2002). Evidence that the tandem-pleckstrin-homology-domain-containing protein TAPP1 interacts with Ptd(3,4)P2 and the multi-PDZ-domain-containing protein MUPP1 in vivo. Biochem. J. *361*, 525–536.

Komiyama, N.H., Watabe, A.M., Carlisle, H.J., Porter, K., Charlesworth, P., Monti, J., Strathdee, D.J., O'Carroll, C.M., Martin, S.J., Morris, R.G., et al. (2002). SynGAP regulates ERK/MAPK signaling, synaptic plasticity, and learning in the complex with postsynaptic density 95 and NMDA receptor. J. Neurosci. *22*, 9721–9732.

Kornau, H.C., Schenker, L.T., Kennedy, M.B., and Seeburg, P.H. (1995). Domain interaction between NMDA receptor subunits and the postsynaptic density protein PSD-95. Science *269*, 1737–1740.

Krapivinsky, G., Krapivinsky, L., Manasian, Y., Ivanov, A., Tyzio, R., Pellegrino, C., Ben-Ari, Y., Clapham, D.E., and Medina, I. (2003). The NMDA receptor is coupled to the ERK pathway by a direct interaction between NR2B and RasGRF1. Neuron *40*, 775–784.

Lau, L.F., Mammen, A., Ehlers, M.D., Kindler, S., Chung, W.J., Garner, C.C., and Huganir, R.L. (1996). Interaction of the N-methyl-D-aspartate receptor complex with a novel synapse-associated protein, SAP102. J. Biol. Chem. *271*, 21622–21628.

Li, W., Okano, A., Tian, Q.B., Nakayama, K., Furihata, T., Nawa, H., and Suzuki, T. (2001). Characterization of a novel synGAP isoform, synGAP-beta. J. Biol. Chem. *276*, 21417–21424.

Lisman, J., Schulman, H., and Cline, H. (2002). The molecular basis of CaMKII function in synaptic and behavioural memory. Nat. Rev. Neurosci. *3*, 175–190.

Lu, W., Man, H., Ju, W., Trimble, W.S., MacDonald, J.F., and Wang, Y.T. (2001). Activation of synaptic NMDA receptors induces membrane insertion of new AMPA receptors and LTP in cultured hippocampal neurons. Neuron *29*, 243–254.

Luo, J., Wang, Y., Yasuda, R.P., Dunah, A.W., and Wolfe, B.B. (1997). The majority of N-methyl-D-aspartate receptor complexes in adult rat cerebral cortex contain at least three different subunits (NR1/NR2A/NR2B). Mol. Pharmacol. *51*, 79–86.

Luscher, C., Xia, H., Beattie, E.C., Carroll, R.C., von Zastrow, M., Malenka, R.C., and Nicoll, R.A. (1999). Role of AMPA receptor cycling in synaptic transmission and plasticity. Neuron *24*, 649–658.

Malinow, R. (2003). AMPA receptor trafficking and long-term potentiation. Philos. Trans. R. Soc. Lond. B. Biol. Sci. *358*, 707–714.

Man, H.Y., Wang, Q.H., Lu, W.Y., Ju, W., Ahmadian, G., Liu, L.D., D'Souza, S., Wong, T.P., Taghibiglou, C., Lu, J., et al. (2003). Activation of P13-kinase is required for AMPA receptor insertion during LTP of mEPSCs in cultured hippocampal neurons. Neuron *38*, 611–624.

Mancini, A., Koch, A., Stefan, M., Niemann, H., and Tamura, T. (2000). The direct association of the multiple PDZ domain containing proteins (MUPP-1) with the human c-Kit C-terminus is regulated by tyrosine kinase activity. FEBS Lett. *482*, 54–58.

Oh, J.S., Chen, H.J., Rojas-Soto, M., Oguni, A., and Kennedy, M.B. (2002). A synaptic ras-GTPase activating protein (p135 SynGAP) inhibited by CaM kinase II. Neuron *33*, 151–151.

Oh, J.S., Manzerra, P., and Kennedy, M.B. (2004). Regulation of the neuron-specific Ras GTPase-activating protein, synGAP, by Ca^{2+}/calmodulin-dependent protein kinase II. J. Biol. Chem. *279*, 17980–17988.

Palsson, E.M., Popoff, M., Thelestam, M., and O'Neill, L.A. (2000). Divergent roles for Ras and Rap in the activation of p38 mitogen-activated protein kinase by interleukin-1. J. Biol. Chem. *275*, 7818–7825.

Park, H.O., Chant, J., and Herskowitz, I. (1993). BUD2 encodes a GTPase-activating protein for Bud1/Rsr1 necessary for proper bud-site selection in yeast. Nature *365*, 269–274.

Parker, L.L., Backstrom, J.R., Sanders-Bush, E., and Shieh, B.H. (2003). Agonist-induced phosphorylation of the serotonin 5-HT2C receptor regulates its interaction with multiple PDZ protein 1. J. Biol. Chem. *278*, 21576–21583.

Pei, L., Teves, R.L., Wallace, M.C., and Gurd, J.W. (2001). Transient cerebral ischemia increases tyrosine phosphorylation of the synaptic RAS-GTPase activating protein, SynGAP. J. Cereb. Blood Flow Metab. *21*, 955–963.

Penzes, P., Johnson, R.C., Sattler, R., Zhang, X., Huganir, R.L., Kambampati, V., Mains, R.E., and Eipper, B.A. (2001). The neuronal Rho-GEF Kalirin-7 interacts with PDZ domain-containing proteins and regulates dendritic morphogenesis. Neuron *29*, 229–242.

Platenik, J., Kuramoto, N., and Yoneda, Y. (2000). Molecular mechanisms associated with long-term consolidation of the NMDA signals. Life Sci. *67*, 335–364.

Poliak, S., Matlis, S., Ullmer, C., Scherer, S.S., and Peles, E. (2002). Distinct claudins and associated PDZ proteins form different autotypic tight junctions in myelinating Schwann cells. J. Cell Biol. *159*, 361–372.

Salojin, K.V., Zhang, J., and Delovitch, T.L. (1999). TCR and CD28 are coupled via ZAP-70 to the activation of the Vav/Rac-1-/PAK-1/p38 MAPK signaling pathway. J. Immunol. *163*, 844–853.

Sheng, M., and Sala, C. (2001). PDZ domains and the organization of supramolecular complexes. Annu. Rev. Neurosci. *24*, 1–29.

Shi, S.H., Hayashi, Y., Petralia, R.S., Zaman, S.H., Wenthold, R.J., Svoboda, K., and Malinow, R. (1999). Rapid spine delivery and redistribution of AMPA receptors after synaptic NMDA receptor activation. Science *284*, 1811–1816.

Sitek, B., Poschmann, G., Schmidtke, K., Ullmer, C., Maskri, L., Andriske, M., Stichel, C.C., Zhu, X.R., and Luebbert, H. (2003). Expression of MUPP1 protein in mouse brain. Brain Res. *970*, 178–187.

Tochio, H., Zhang, Q., Mandal, P., Li, M., and Zhang, M. (1999). Solution structure of the extended neuronal nitric oxide synthase PDZ domain complexed with an associated peptide. Nat. Struct. Biol. *6*, 417–421.

Tomoda, T., Kim, J.H., Zhan, C., and Hatten, M.E. (2004). Role of Unc51.1 and its binding partners in CNS axon outgrowth. Genes Dev. *18*, 541–558.

Ullmer, C., Schmuck, K., Figge, A., and Lubbert, H. (1998). Cloning and characterization of MUPP1, a novel PDZ domain protein. FEBS Lett. *424*, 63–68.

Wadia, J.S., and Dowdy, S.F. (2003). Modulation of cellular function by TAT mediated transduction of full length proteins. Curr. Protein Pept. Sci. *4*, 97–104.

Xu, G.F., Lin, B., Tanaka, K., Dunn, D., Wood, D., Gesteland, R., White, R., Weiss, R., and Tamanoi, F. (1990). The catalytic domain of the neurofibromatosis type 1 gene product stimulates ras GTPase and complements ira mutants of *S. cerevisiae*. Cell *63*, 835–841.

Zhu, J.J., Qin, Y., Zhao, M., Van Aelst, L., and Malinow, R. (2002). Ras and Rap control AMPA receptor trafficking during synaptic plasticity. Cell *110*, 443–455.